Physics and Astronomy Department
4400 University Drive 6C3
Fairfax, VA 22030
Tel: +1 703 225-9080; Fax: +1 703 993-1296
tduxbury@gmu.edu

Mariner Mars 1969 Near Encounter Analytic Geometric Camera Model: the basis for a NAIF SPICE Instrument Kernel

Thomas C. Duxbury
Physics and Astronomy Department
George Mason University
Fairfax, VA 22030 USA
(tduxbury@gmu.edu)
Prepared for *NASA PDART*, 18 November 2019

Physics and Astronomy Department
4400 University Drive 6C3
Fairfax, VA 22030
Tel: +1 703 225-9080; Fax: +1 703 993-1296
tduxbury@gmu.edu

1 Introduction

The Mariner Mars 1969 Mission had two spacecraft, Mariner 6 and Mariner 7, each carrying a narrow and a wide angle camera. The Wide Angle (WA) cameras had Zeiss refractor optics with shutters that incorporated four spectral filters in a rotary wheel in the order red, green, blue and green again. The Narrow Angle (NA) cameras had Schmidt-Cassegrain reflector optics without filters. The wide angle f/5.6 lenses had focal lengths of about 52.5 mm and the narrow angle f/2.4 lenses had focal lengths of about 504 mm. The optics focused images onto vidicons to obtain images of Mars. The vidicons were etched with 7 x 9 grids of reseaux to aid in computing the geometric distortions in the digital images. All four cameras produced 945 sample by 704 line, 8 bit/pixel digital images after ground processing to produce the Experiment Data Record image archive. Unlike Far Encounter, a complete set of Near Encounter raw (distorted) 945 sample by 704 line images was not found to process. Therefore, the complete set of distortion corrected 1000 sample x 772 line images was used to create the Camera Models in the NAIF SPICE Instrument Kernels. The NAIF SPICE spacecraft and camera identification numbers are given in Table 1.

A generic analytic geometric camera model is presented for the Near Encounter images to map from object space, through the optics onto the vidicon focal plane and then to the digital image coordinates, that is applicable to all four cameras. The image coordinates of the reseau grid need to be measured in each Near Encounter image to determine the vidicon geometric model parameter values that change from image to image. For a given image, the geometric model is accurate at the few pixel level. For more precision, extra corrections need to be added to the geometric model, for example, by a bi-linear interpolation process between reseaux surrounding a vidicon location.

To validate the analytic model, the Mariner 6 and 7 Near Encounter images were processed to determine the camera model parameter values as part of the second year effort of a NASA Planetary Data Archive, Restoration and Technology (PDART) task. Far Encounter only contained Narrow Angles images. Both Narrow Angle and Wide Angle images were obtained in the Near Encounter mission phases. The derived models identified 4 of the Near Encounter images that had missing lines that could not be recovered.

2 Near Encounter Geometric Camera Model

The Near Encounter geometric model for the 1969 Mariner 6 and 7 NA and WA cameras includes terms for the optics and additional terms for the vidicon that are needed to predict the image coordinates of celestial objects, such as Mars limb and surface features that are outside of the camera optics, and also to predict the image coordinates of the grids of reseaux that are etched into the vidicon photo sensitive surfaces. The measured image coordinates of the reseau grid are used to determine the vidicon geometric parameters while simulated images were overlain on the actual images to determine the optical geometric parameters.

To define the geometric camera model, a Mars centered and fixed position $\bar{\mathbf{u}}$ of a surface feature on Mars is projected through the optics, onto the vidicon and then into image coordinates. A surface feature on Mars is defined by its Mars-centered and fixed cartographic coordinates of latitude, ϕ, longitude, λ, and radius, r, relative to the Mars equator and equinox of date reference system $\mathbf{X}, \mathbf{Y}, \mathbf{Z}$

Physics and Astronomy Department
4400 University Drive 6C3
Fairfax, VA 22030
Tel: +1 703 225-9080; Fax: +1 703 993-1296
tduxbury@gmu.edu

$$\begin{bmatrix} u_X \\ u_Y \\ u_Z \end{bmatrix} = \bar{\mathbf{u}} = r\hat{\mathbf{u}} = r \begin{bmatrix} \cos\phi \ \cos\lambda \\ \cos\phi \ \sin\lambda \\ \sin\phi \end{bmatrix} \quad \text{(km)} \tag{1}$$

where u_x, u_y, u_z are the position components of the surface feature position vector $\hat{\mathbf{u}}$ in Mars centered and fixed coordinates and $\hat{\mathbf{u}}$ is the Mars-center and fixed unit direction vector to the surface feature. The Mars-centered vector $\hat{\mathbf{u}}$ is translated to a Mariner Mars 1969 spacecraft-centered and Mars-fixed position vector using the Mars-centered and fixed position vector $\bar{\mathbf{w}}$ of the spacecraft and then transformed from spacecraft-fixed to camera centered and fixed position vector $\bar{\mathbf{p}}$ using

$$\begin{bmatrix} p_x \\ p_y \\ p_z \end{bmatrix} = \bar{\mathbf{p}} = \mathbf{C}\,(\mathbf{u} - \mathbf{w}) \quad \text{(km)} \tag{2}$$

where p_x, p_y, p_z are the position components of the camera-centered and fixed surface feature position vector $\bar{\mathbf{p}}$ and $\mathbf{C}$ is the transformation from Mars-fixed to camera-fixed coordinates, a SPICE C kernel.

A camera-fixed, $\bar{\mathbf{x}}\bar{\mathbf{y}}\bar{\mathbf{z}}$ coordinate system is defined in the Mariner 6 and 7, Wide and Narrow Angle vidicon focal planes with axis $\bar{\mathbf{x}}$ is in the direction of increasing sample number, axis $\bar{\mathbf{y}}$ is in the direction of increasing line number and axis $\bar{\mathbf{z}}$ completing the orthogonal right-handed system and is in the direction of the optical axis (Figure 1). For each Mariner Mars 1969 vidicon detector, the origin of $\bar{\mathbf{x}}\bar{\mathbf{y}}\bar{\mathbf{z}}$ is placed at their central reseaux. The geometric camera model is developed in terms of an optical component and a vidicon component that are described in the next sub-sections.

2.1 Optics Model

A camera-fixed vector $\bar{\mathbf{p}}$ in $\bar{\mathbf{x}}\bar{\mathbf{y}}\bar{\mathbf{z}}$ to a surface feature can be mapped through the optics into the camera-fixed, undistorted vidicon focal plane coordinates x, y using the following set of analytic equations based upon the co-linear equations of photogrammetry (Thompson, 1966, Figure 1)

$$\begin{bmatrix} x \\ y \end{bmatrix} = \frac{f}{p_z} \begin{bmatrix} p_x \\ p_y \end{bmatrix} \quad \text{(mm)} \tag{3}$$

where f is the camera focal length (mm) and $p_x,\ p_y,\ p_z$ are the position components to the surface feature in camera-fixed $\bar{\mathbf{x}}\bar{\mathbf{y}}\bar{\mathbf{z}}$ coordinates. Optics produce distortions in the radial direction, especially for larger fields-of-view, that deflect the undistorted focal plane coordinates x, y in equation 3 into optically distorted focal plane coordinates x', y' that are modeled by

$$\begin{bmatrix} x' \\ y' \end{bmatrix} = \begin{bmatrix} x \\ y \end{bmatrix} + \alpha_1 \begin{bmatrix} o_x \\ o_y \end{bmatrix} r_o^2 + \alpha_2 \begin{bmatrix} o_x \\ o_y \end{bmatrix} r_o^4 \quad \text{(mm)} \tag{4}$$

where x', y' are the actual focal plane, optically distorted, coordinates on the vidicon,

$$o_x = x - x_o; \quad o_y = y - y_o; \quad r_o^2 = o_x^2 + o_y^2 \tag{5}$$

Physics and Astronomy Department
4400 University Drive 6C3
Fairfax, VA 22030
Tel: +1 703 225-9080; Fax: +1 703 993-1296
tduxbury@gmu.edu

and x_o, y_o are the focal plane coordinates of the optical principal point, the center of the optical distortion relative to the central reseau. The distance r' of the optically distorted vidicon location x', y' from the central reseau is

$$r' = \sqrt{x'^2 + y'2} \tag{6}$$

The terms $f, x_o, y_o, \alpha_1, \alpha_2$ make up the optics contribution to the geometric camera model. The camera-fixed direction vector that gives optically distorted focal plane coordinates of the principal point, x_o, y_o, is used to define camera pointing. The known positions of Mars-fixed surface features seen in the images are used to determine the optical model parameter values. The values for the Near Encounter Optical Model parameters are listed in Table 7.

2.2 Vidicon Model

Given the optical distorted focal plane coordinates x', y' in equation 4, the image coordinates of sample, s, and line, l, can be computed for the direction vector $\hat{\mathbf{p}}$ in $\bar{\mathbf{x}}\bar{\mathbf{y}}\bar{\mathbf{z}}$ from

$$\begin{bmatrix} s \\ l \end{bmatrix} = \begin{bmatrix} K_{sx} & K_{sy} \\ K_{lx} & K_{ly} \end{bmatrix} \begin{bmatrix} x' \\ y' \end{bmatrix} + \begin{bmatrix} s_0 \\ l_0 \end{bmatrix} \quad \text{(pixels)} \tag{7}$$

where the K's are scale factors mapping between optical distorted focal plane coordinates of mm to image coordinates of s, l and s_0, l_0 are the sample and line image coordinates of the central reseau, the origin of the camera-fixed coordinate system. For all distortion corrected level-2 archived images from all four cameras

$$1 \leq s \leq 1,000 \quad \text{and} \quad 1 \leq l \leq 772 \tag{8}$$

The K, s_0, l_0 terms comprise the vidicon contribution to the geometric camera model.

The Mariner 6 and 7 Narrow and Wide Angle camera geometric model (equations 3 - 7) for all Near Encounter images is defined by the values of $f, x_o, y_o, \alpha_1, \alpha_2, K_{sx}, K_{sy}, K_{lx}, K_{ly}, s_0$ and l_0. The following sections describe how the values for these parameters were determined from the Near Encounter images for all four cameras. The values of s_0, l_0 are determined directly from the s, l image coordinates of the central reseau in each image. The values for the Mariner 6 and 7 Narrow and Wide Angle Camera Near Encounter Vidicon Model parameters are listed in Tables 3 - 6, respectively.

3 Reseau Grid

As a direct aid in determining the $K's, s_0$ and l_0, a 7 x 9 grid of reseaux was etched onto each vidicon and the actual focal plane x', y' coordinates in equation 3 of each reseau were measured for each vidicon (Figure 2). Note that the direction of $+\mathbf{y}$ in this figure is opposite to the convention used here and therefore the negative of the y coordinates shown in Figure 2 was used in equation 7. Unfortunately, the focal plane coordinates for only the Mariner 6 Wide Angle vidicon reseaux were found (Table 1. - Danielson and Montgomery, 1971). Therefore for the remainder of these analyses, it is assumed that all four vidicons have the same reseau grid focal plane coordinates as shown in Figure 2. With K_{sx} and K_{ly} being about 75 pixels / mm, it is expected that any errors made by this assumption will be at the 1 pixel level across all vidicons. Four of the images had values for K_{ly} that were many lines / mm lower than the nominal values that indicated that there were missing lines in the images and these missing lines were not recoverable.

GEORGE MASON UNIVERSITY
Physics and Astronomy Department
4400 University Drive 6C3
Fairfax, VA 22030
Tel: +1 703 225-9080; Fax: +1 703 993-1296
tduxbury@gmu.edu

From equation 7, it is seen that observing the image coordinates of the reseau grid would yield the vidicon geometric parameters $K_{sx}, K_{sy}, K_{lx}, K_{ly}, s_0$ and l_0. As mentioned previously, the reseau grid needs to be measured in each image for model fidelity as the vidicon readout distortions change from image to image at more than one pixel.

4 Linear Partial Derivative Equations

A weighted, least-squares, minimum variance, square-root parameters estimation technique (Beirman, 1977) was used to determine the optical and vidicon geometric camera model parameter values. The s, l image coordinates of known Martian surface features and the reseaux were measured in the distortion corrected (level-2) images and used as the observables in the estimation process. The linear equations used in the estimation process were derived from the partial derivatives of s, l with respect to the estimated parameters. The following gives the derivation of these linear, partial derivative expressions used to form the linear equations for each observed surface feature and reseau image location.

$$\frac{\partial(s,l)}{\partial(K_{sx},K_{sy},K_{lx},K_{ly})} = \begin{bmatrix} x' & y' & 0 & 0 \\ 0 & 0 & x' & y' \end{bmatrix} \tag{9}$$

$$\frac{\partial(s,l)}{\partial(s_0,l_0)} = \begin{bmatrix} 1 & 0 \\ 0 & 1 \end{bmatrix} \tag{10}$$

$$\frac{\partial(s,l)}{\partial(x',y')} = \begin{bmatrix} K_{sx} & K_{sy} & 0 & 0 \\ 0 & 0 & K_{lx} & K_{ly} \end{bmatrix} \tag{11}$$

$$\frac{\partial(x',y')}{\partial(\alpha_1,\alpha_2)} = \begin{bmatrix} o_x r_o^2 & o_x r_o^4 \\ o_y r_o^2 & o_y r_o^4 \end{bmatrix} \tag{12}$$

$$\frac{\partial(x',y')}{\partial(x)} = \begin{bmatrix} 1+\alpha_1\ r_o^2 + 2\alpha_1\ o_x^2 + \alpha_2\ r_o^4 + 4\alpha_2\ o_x^2\ r_o^2 \\ 2\alpha_1\ o_x\ o_y + 4\alpha_2\ o_x\ o_y\ r_o^2 \end{bmatrix} \tag{13}$$

$$\frac{\partial(x',y')}{\partial(y)} = \begin{bmatrix} 2\alpha_1\ o_x\ o_y + 4\alpha_2\ o_x\ o_y\ r_o^2 \\ 1+\alpha_1\ r_o^2 + 2\alpha_1\ o_y^2 + \alpha_2\ r_o^4 + 4\alpha_2\ o_y^2\ r_o^2 \end{bmatrix} \tag{14}$$

$$\frac{\partial(x',y')}{\partial(o_x)} = \begin{bmatrix} -\alpha_1\ r_o^2 + 2\alpha_1\ o_x^2 - \alpha_2\ r_o^4 + 4\alpha_2\ o_x^2\ r_o^2 \\ 2\alpha_1\ o_x\ o_y + 4\alpha_2\ o_x\ o_y\ r_o^2 \end{bmatrix} \tag{15}$$

$$\frac{\partial(x',y')}{\partial(o_y)} = \begin{bmatrix} 2\alpha_1\ o_x\ o_y + 4\alpha_2\ o_x\ o_y\ r_o^2 \\ -\alpha_1\ r_o^2 + 2\alpha_1\ o_y^2 - \alpha_2\ r_o^4 + 4\alpha_2\ o_y^2\ r_o^2 \end{bmatrix} \tag{16}$$

$$\frac{\partial(x,y)}{\partial(p_x,p_y,p_z,f)} = \frac{1}{p_z}\begin{bmatrix} f & 0 & -x & p_x \\ 0 & f & -y & p_y \end{bmatrix} \tag{17}$$

Physics and Astronomy Department
4400 University Drive 6C3
Fairfax, VA 22030
Tel: +1 703 225-9080; Fax: +1 703 993-1296
tduxbury@gmu.edu

Equations 12 - 25 can be combined using the chain rule to form the $\partial(s,l)$ with respect to the $\partial(p_x, p_y, p_z, f, x_o, y_o, \alpha_1, \alpha_2, K_{sx}, K_{sy}, K_{lx}, K_{ly}, x_v, y_v, \beta_0, \beta_2, \gamma_0, \gamma_2, s_0, l_0)$ to be used as the linear equation in the estimation process.

$$\frac{\partial(s,l)}{\partial(p_x,p_y,p_z,f)} = \frac{\partial(s,l)}{\partial(x',y')}\frac{\partial(x',y')}{\partial(x,y)}\frac{\partial(x,y)}{\partial(p_x,p_y,p_z,f)} \tag{18}$$

$$\frac{\partial(s,l)}{\partial(o_x,o_y)} = \frac{\partial(s,l)}{\partial(x',y')}\frac{\partial(x',y')}{\partial(o_x,o_y)} \tag{19}$$

$$\frac{\partial(s,l)}{\partial(\alpha_1,\alpha_2)} = \frac{\partial(s,l)}{\partial(x',y')}\frac{\partial(x',y')}{\partial(\alpha_1,\alpha_2)} \tag{20}$$

Table 2 lists the analytic partial derivatives and the differenced partial derivatives for reseaux in the upper left corner in an image. The center two columns are for the sample partial derivative comparisons and the right two columns are for the line partial derivation comparisons. The partial derivatives are only dependent on image location and not for any specific image. This comparison validates the analytic partial derivatives to better than 0.1%, sufficient for this data analysis.

It is noted that the p_x, p_y, p_z terms in equation 2 are used for objects outside of the cameras such as Mars surface features that are used to compute camera optical model parameters.

5 Mariner 6 and 7 Near Encounter Vidicon Parameter Values

There were up to 10 versions of each Near Encounter image but only 6 that could be considered for restoration and archive (Figure 4). The best versions of the Near Encounter images to restore were found to be those that were distortion corrected. These had the reseaux intact that were needed to compute the vidicon geometric model, the least missing lines, the least artifacts, the most discernible views of the surface and were all 1,000 samples per line and 772 lines.

To measure the image locations of the reseaux to determine the vidicon model parameter values, each Near Encounter image was high-pass filtered to accentuate the reseaux. Figure 3 shows the original 6N11 image (left) and a high-pass filtered version of the image (right). Reseux were observable when against a Mars background but were not visible off of the Mars limb against the dark space background. Even with a Mars background, not all reseaux were observed, especially those on the masks surrounding the active image area. Therefore, depending on the image content, as few as 21 and as many as 62 of the 63 reseaux were observed in an image.

Five different filter weights (Weiner, 1949) were used to automatically measure the reseaux locations: at the top; on the left mask; in the center; on the right mask; on the bottom left; and on the bottom right of the images. Figure 5 shows these filter weights of the central 5 x 5 areas of 7x7 digital filters used to autocorrelate with each type of reseau. The filter weights outside of the central 5 x 5 area were all equal to a negative value such that the sum of all filter weights within the 7 x 7 area was zero. Some of the bottom reseaux were not on the bottom mask and the center filter weights were used rather than the left or right bottom weights.

The images chosen to restore were distortion corrected; however there was no documentation that gave information on the geometrics of these distortion corrected images. Therefore the reseau

Physics and Astronomy Department
4400 University Drive 6C3
Fairfax, VA 22030
Tel: +1 703 225-9080; Fax: +1 703 993-1296
tduxbury@gmu.edu

locations were measured in all Near Encounter images to compute the vidicon geometric parameter values. Since the major distortions were removed from these images, only the parameter values for $K_{sx}, K_{sy}, K_{lx}, K_{ly}, s_0$ and l_0 were determined for the vidicon model of each image. It was assumed that all images from each of the 4 cameras should have similar vidicon geometric parameter values and therefore the vidicon models were grouped by camera.

To start the least-squares parameter estimation process, *a priori* values of K_{sx} and K_{ly} for each camera were determined from the slopes of the reseau locations in sample / line versus their focal plane mm locations (Figures 6 - 9). It is seen that the image scales are between 73 - 75 pixels / mm. Almost all images with missing lines were zero-filled where the lines were missing. However in a few of the images, missing lines were not zero-filled where the lines were missing but lines were added to the ends of these images to keep the files 772 lines. long. For these images, bogus image line locations in 6N11, 6N12, 7N23 and 7N24 were measured and the values determined for K_{ly} were smaller by a few lines/mm than the full frame images. No data were located to determine the missing lines; therefore no attempt was made to find and fill in the missing lines and correct the values for K_{ly}.

The *a priori* values of K_{sy} and K_{lx} were zero. The *a priori* values used for s_0, l_0 were the observed image locations of the central reseau in each picture. For each iteration, *a priori* 1-σ parameter uncertainties of 0.5 pixels/mm was used for the K terms. The *a priori* 1-σ uncertainties of the locations of the central reseaux were 0.1 pixels since their locations were measured directly.

Tables 3. - 7. list the vidicon parameter values for all Mariner 6 and 7, Wide and Narrow Angle Near Encounter images. Average values for each camera are the last entry in each table. As mentioned, images 6N23, 6N24, 7N11 and 7N12 have missing lines, giving erroneous values for K_{ly}. The parameter values for these images are not included in the average camera vidicon geometric parameter values. These average parameter values are also included in the SPICE Instrument kernel mr69_ne_camera_vidicon_model_catalog.tab that are part of the Mariner Mars 1969 Bundle Archive. Additionally the observed reseau locations in each image and their differences with their predicted locations are in the file mr69_ne_reseau_catalog.tab, also included in the Mariner Mars 1969 Bundle Archive. The post-fit reseau location residual statistics, the difference between the observed and predicted locations, were about 1 pixel (1σ) or less . Figure 10 shows the observed reseau locations within the circles for 6N17 and the residuals, scaled by a factor of 20, as line emanating from the circle centers. The two orthogonal scale bars in the image center are 2 pixels in length.

6 Optical Model Parameter Values

The camera optical parameter values listed in Table 7 were determined by mapping the MOLA global digital terrain model (DTM) into each image using equations 1 - 7. The vidicon parameter values used are listed in Tables 3 - 7. For the optical parameters, the pre-launch focal length values of 505.41 mm and 502.66 mm for the Mariner 6 and 7 Narrow Angle cameras, respectively, and 52.03 mm and 52.56 mm for the Mariner 6 and 7 Wide Angle cameras, respectively (Danielson and Montgomery, 1971), were used. The optical principal points location values were zero. The MOLA DTM was registered to each image by changing the clock α and cone β angles. These clock and cone angles that achieved registration of the MOLA image to the actual image are captured in the camera pointing NAIF SPICE C kernels and are listed in Tables 8 - 11.

Physics and Astronomy Department
4400 University Drive 6C3
Fairfax, VA 22030
Tel: +1 703 225-9080; Fax: +1 703 993-1296
tduxbury@gmu.edu

This registration process is demonstrated in Figures 11 and 12. In Figure 11, the MOLA DTM is mapped into image coordinates (right) using the camera vidicon and optical parameters described in the previous paragraph and the nominal camera pointing angles. When the MOLA image is overlain on the actual image (Figure 12 - left), there is a mis-registration. The camera pointing clock and cone angles are changed until registration is achieved (Figure 12 - right). It is seen that the registration is achieved across this entire Wide Angle camera image, validating the pre-launch camera optical parameter values. This was the case for all 4 cameras.

These optical and vidicon geometric parameters and their values are used to create NAIF SPICE Instrument Kernels (IK - Acton, 1996 and Acton, *et. al.*, 2017) for the Mariner 6 and 7 Narrow Angle cameras.

References

[*Acton*(1996)] Acton, C. H. (1996), Ancillary data services of NASA's Navigation and Ancillary Information Facility, *Planetary & Space Sci.*, *44*, 1, 65-70.

[*Acton et al*(2017)] Acton, C., N. Bachman, B. Semenov, and E. Wright; A look toward the future in the handling of space science mission geometry (2017); *Planetary & Space Sci.*, *DOI 10.1016/j.pss.2017.02.013*.

[*Bierman*(1977)] Bierman, G. J., Factorization methods for discrete sequential estimation (1977), Mathematics in Science and Engineering, Volume *1*28, 241 pages, *A*cademic Press, New York, NY.

[*Collins*(1971)] Collins, S. A. (1971), The Mariner 6 and 7 pictures of Mars, *NASA SP*, *263*, Washington, D. C.

[*Danielson & Montgomery.*(1971)] Danielson, G. E. and D. R. Montgomery (1971), Calibration of the Mariner Mars 1969 Television Cameras, *J. Geophys. Res.*, *76*, 2, 418 - 431, doi: 10.1029/JB076i002p00418.

[*Leighton et al*(1969)] Leighton, R. B., N. H. Horowitz, B. C. Murray, R. P. Sharp, A. H. Herriman, A. T. Young, B. A. Smith, M. E. Davies and C. B. Leovy (1969), Mariner 6 and 7 Television Pictures; Preliminary Analysis , *Science*, *166*, 3901, 49 - 67, ISSN 0036-8075.

[*Leighton et al*(1971)] Leighton, R. B and B. C. Murray (1971), One year's processing and interpretation - An overview, *J. Geophys. Res.*, *76*, 2, 293 - 296, doi:10.1029/JB076i002p00293.

[*MM69*(1996)] Mariner-Mars 1969, A Preliminary Report, (1969), *NASA SP*, *225*, Washington, D. C.

[*MM69 Handbook*(1996)] Mariner Mars 1969 Handbook (MARINER VI & VII), (July 28, 1969), *Jet Propulsion Laboratory*, *605-211*, California Institute of Technology.

[*Rindfleisch et al*(1971)] Rindfleisch, T. C., J. A. Dunne, H. J. Frieden, W. D. Stromberg and R. M. Ruiz (1971), Digital Processing of the Mariner Mars 1969 Pictures, *J. Geophys. Res.*, *76*, 2, 394 - 417, doi:10.1029/JB076i002p00394.

[*Thompson*(1966)] Thompson, M. M. (1966), Ed. *Manual of Photogrammetry*, Third Edition. Falls Church, VA: American Soc. of Photogrammetry.

Physics and Astronomy Department
4400 University Drive 6C3
Fairfax, VA 22030
Tel: +1 703 225-9080; Fax: +1 703 993-129
tduxbury@gmu.edu

[*Weiner*(1949)] Wiener, N. (1949), Extrapolation, interpolation, and smoothing of stationary time series. *New York: Wiley*, *ISBN* 0-262-73005-7.

Physics and Astronomy Department
4400 University Drive 6C3
Fairfax, VA 22030
Tel: +1 703 225-9080; Fax: +1 703 993-1296
tduxbury@gmu.edu

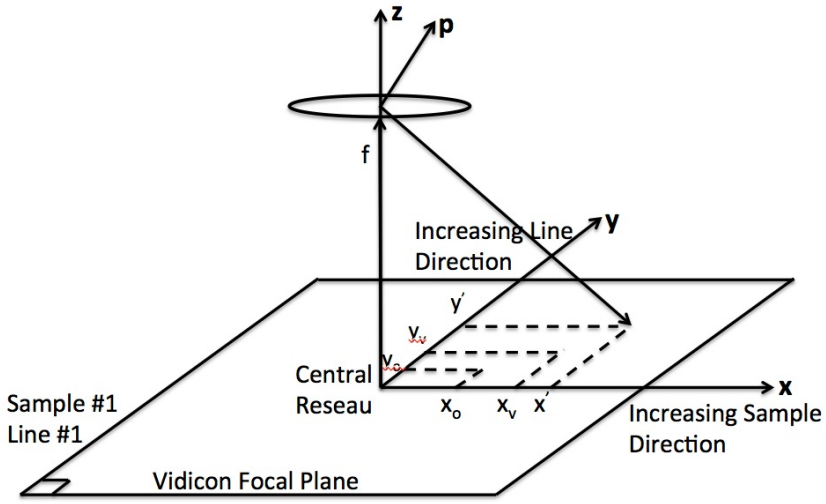

Figure 1: The vidicon-fixed focal plane $\bar{\mathbf{x}}\bar{\mathbf{y}}\bar{\mathbf{z}}$ coordinate system showing an optical system having a focal length f an optical principal point x_0, y_0, a vidicon distortion center at x_v, y_v and an undistorted image location for the camera fixed vector to an object $\mathbf{p}$ at x, y.

Physics and Astronomy Department
4400 University Drive 6C3
Fairfax, VA 22030
Tel: +1 703 225-9080; Fax: +1 703 993-1296
tduxbury@gmu.edu

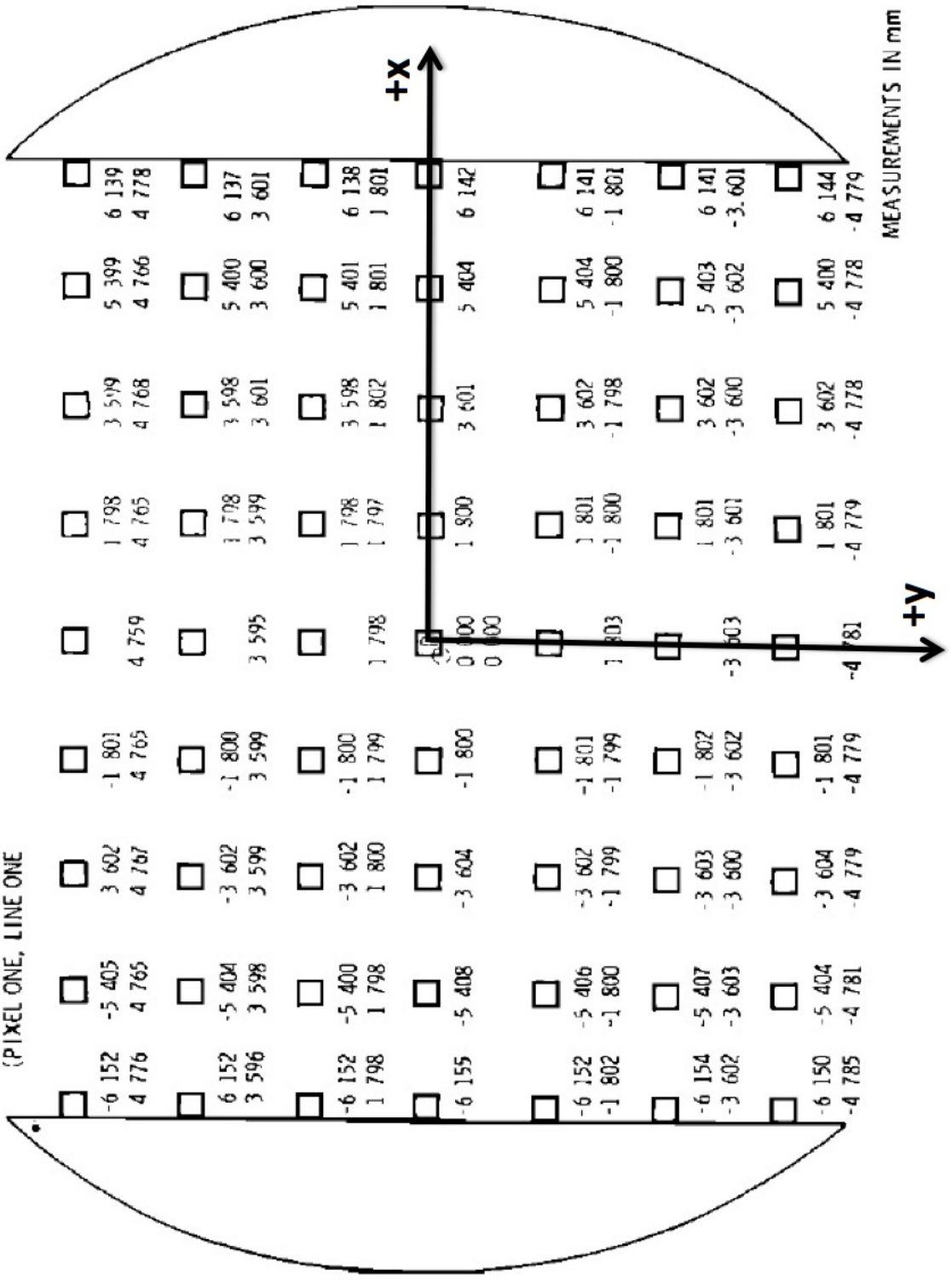

Figure 2: A reseau grid was etched onto each vidicon. NOTE: the y coordinates are reversed in sign.

Physics and Astronomy Department
4400 University Drive 6C3
Fairfax, VA 22030
Tel: +1 703 225-9080; Fax: +1 703 993-1296
tduxbury@gmu.edu

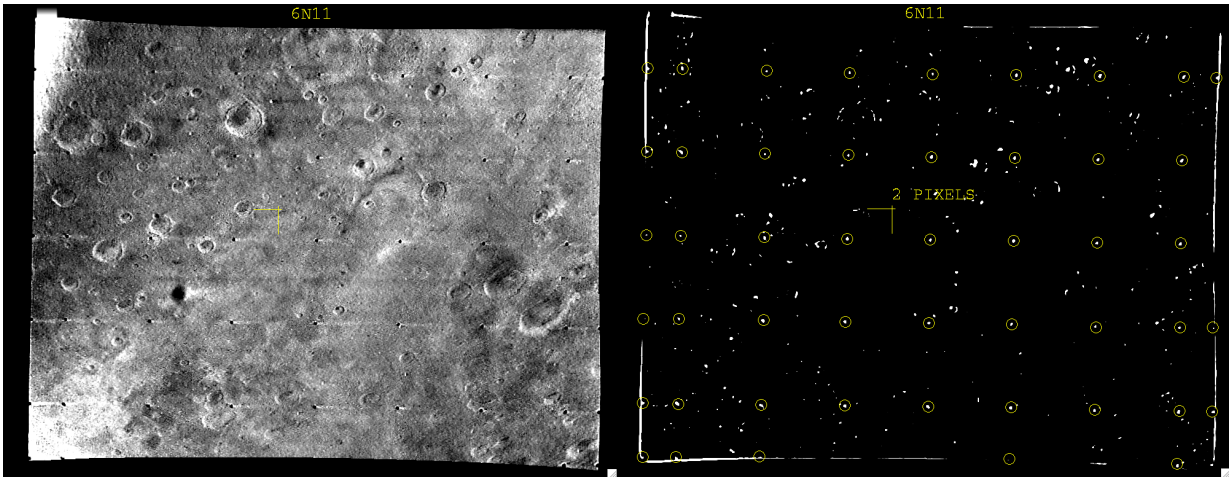

Figure 3: A raw image (6N11 - left) is high pass filtered (right) to enhance the visibility / measurability of the reseau grid inside the yellow circles.

Table 1: Mariner Mars 1969 SPICE Spacecraft and Camera Identification Numbers

S/C	S/C (S & SCLK) Kernels	S/C (C, F & I) Kernels	Narrow Angle Camera	Wide Angle Camera
Mariner 6	-530	-530000	-530101	-530102
Mariner 7	-531	-531000	-531101	-531102

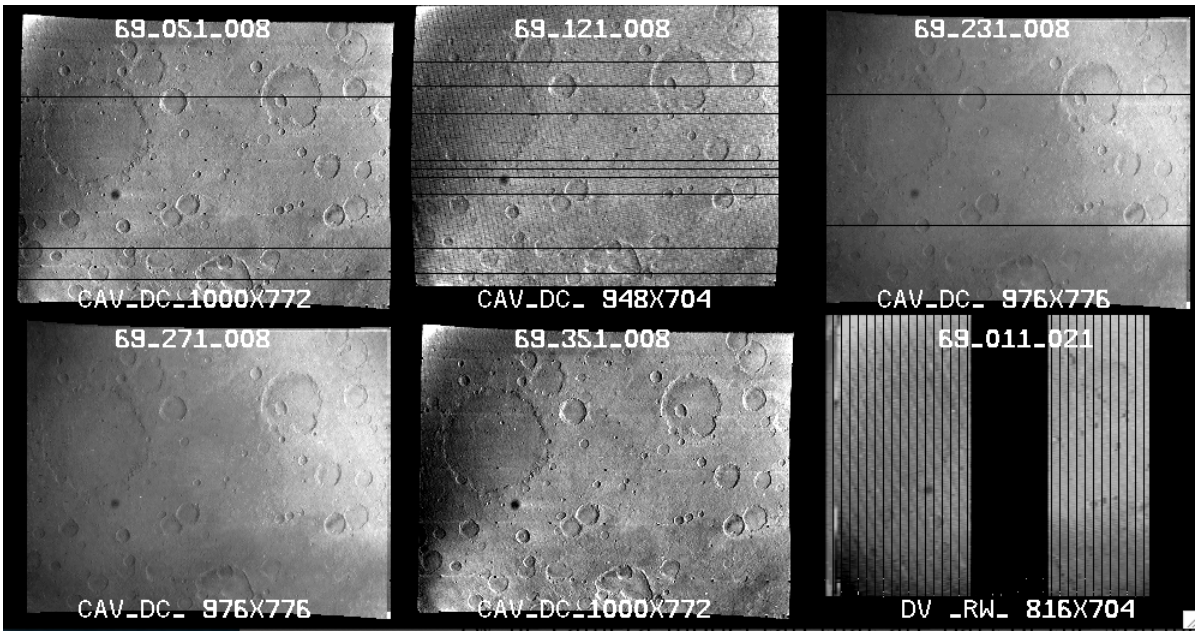

Figure 4: The PDS-supplied CD-ROM, that held the Mariner Mars 1969 images as bmp files, had up to 6 versions of each image. Most were distortion corrected but with the reseaux removed. The file sizes varied significantly. Some had missing lines that were not zero-filled. Some had all lines but only every 7^{th} sample. Fortunately each image had a 1,000 sample x 772 line version with the reseaux intact.

Physics and Astronomy Department
4400 University Drive 6C3
Fairfax, VA 22030
Tel: +1 703 225-9080; Fax: +1 703 993-1296
tduxbury@gmu.edu

TOP

0	0	0	0	0	0	0
0	0	0	0	0	0	0
0	0	0	0	0	0	0
19	5	5	2	4	9	6
117	44	45	19	50	136	128
154	98	94	77	99	128	142
156	137	139	142	138	126	140

LEFT MASK

2	8	14	2	42	158	249
3	9	16	3	34	115	182
2	13	21	0	0	1	2
1	11	17	0	0	0	0
1	4	6	0	0	8	18
0	6	9	1	13	57	107
0	12	20	5	55	153	223

CENTER

174	162	139	142	155	161	139
184	149	71	58	102	148	142
158	109	27	11	56	142	169
144	95	16	2	45	145	182
141	119	43	19	69	145	164
157	152	117	100	129	157	153
151	146	143	149	165	162	143

RIGHT MASK

246	252	235	54	0	0	0
202	118	71	15	0	0	0
119	26	2	0	0	0	0
75	6	0	0	0	0	0
56	5	1	0	0	0	0
95	76	93	12	0	0	0
145	155	188	20	0	0	0

BOTTOM LEFT

248	254	254	252	253	255	252
243	199	163	146	171	222	254
233	105	33	17	68	183	251
0	0	0	0	0	0	0
0	0	0	0	0	0	0
0	0	0	0	0	0	0
0	0	0	0	0	0	0

BOTTOM RIGHT

161	191	195	163	149	160	158
183	203	184	122	98	138	165
189	156	93	45	40	95	155
182	150	90	43	38	91	150
176	145	87	42	37	88	145
170	140	84	40	36	85	140
164	135	81	39	34	82	135

Figure 5: Digital image brightness numbers used to match the six shapes of reseaux. These numbers filled the central 5 x 5 areas of 7 x 7 digital filters used to measure the reseau locations. The numbers outside of the central 5 x 5 areas were constant values such as the sum of the entire 7 x 7 area numbers was zero.

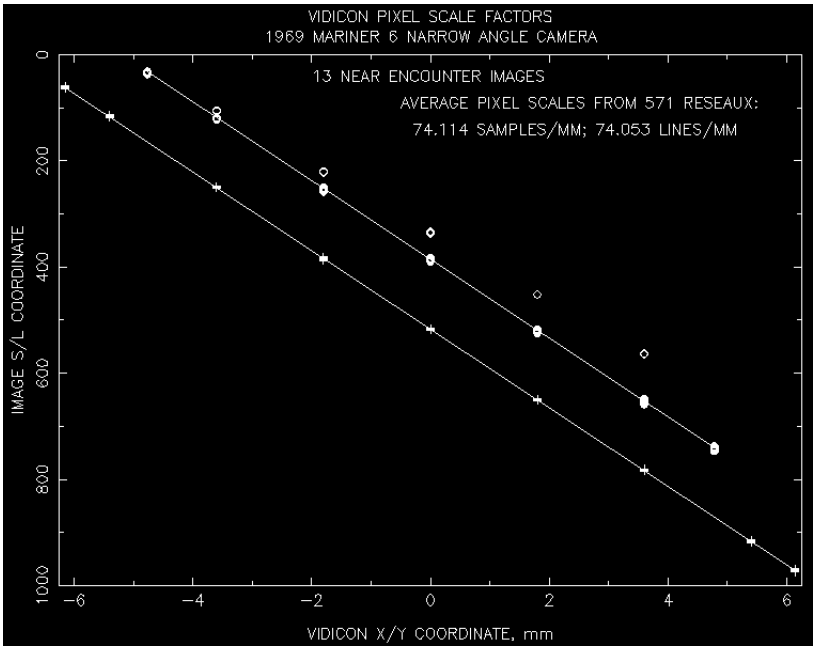

Figure 6: The Mariner 6 Near Encounter Narrow Angle reseau sample/line image coordinates were plotted against their x,y mm focal plane locations to determine *a priori* values of K_{sx}, and K_{ly}. Image 6N24 is missing lines that gives its reseaux erroneous image locations that show up as outliers in the upper data used for line scale.

Physics and Astronomy Department
4400 University Drive 6C3
Fairfax, VA 22030
Tel: +1 703 225-9080; Fax: +1 703 993-1296
tduxbury@gmu.edu

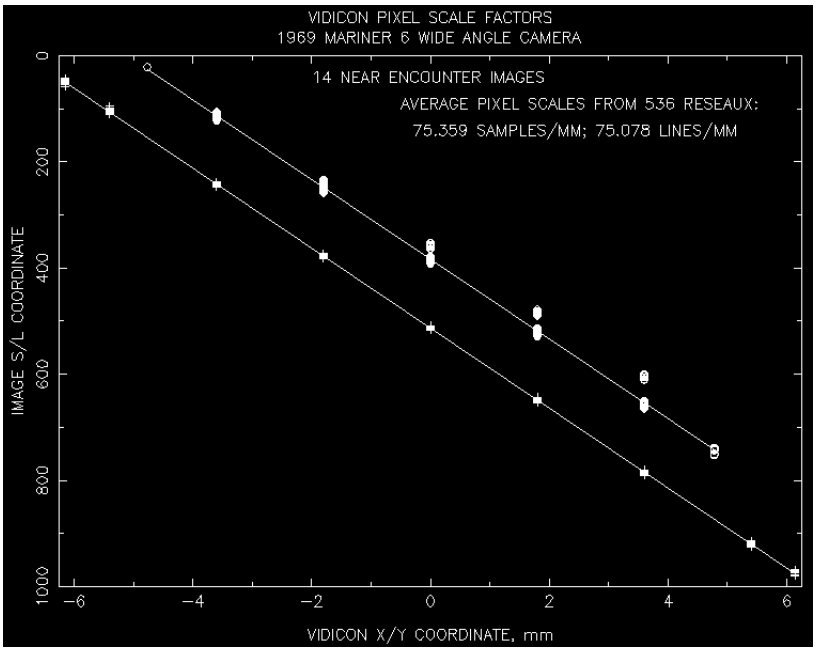

Figure 7: The Mariner 6 Near Encounter Wide Angle reseau sample/line image coordinates were plotted against their x,y mm focal plane locations to determine *a priori* values of K_{sx} and K_{ly}. Image 6N23 is missing lines that gives its reseaux erroneous image locations that show up as outliers in the upper data used for line scale.

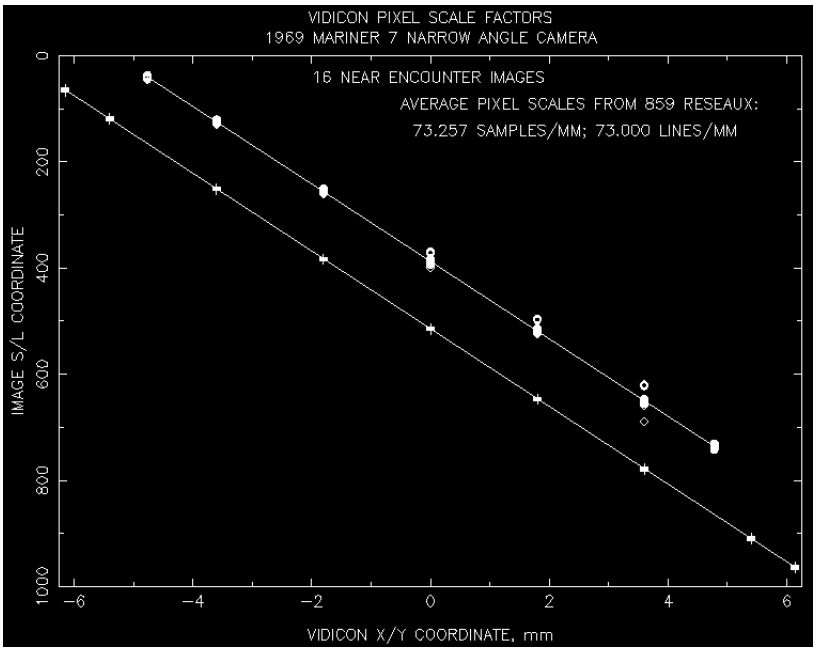

Figure 8: The Mariner 7 Near Encounter Narrow Angle reseau sample/line image coordinates were plotted against their x,y mm focal plane locations to determine *a priori* values of K_{sx} and K_{ly}. Image 7N12 is missing lines that gives its reseaux erroneous image locations that show up as outliers in the upper data used for line scale.

Physics and Astronomy Department
4400 University Drive 6C3
Fairfax, VA 22030
Tel: +1 703 225-9080; Fax: +1 703 993-1296
tduxbury@gmu.edu

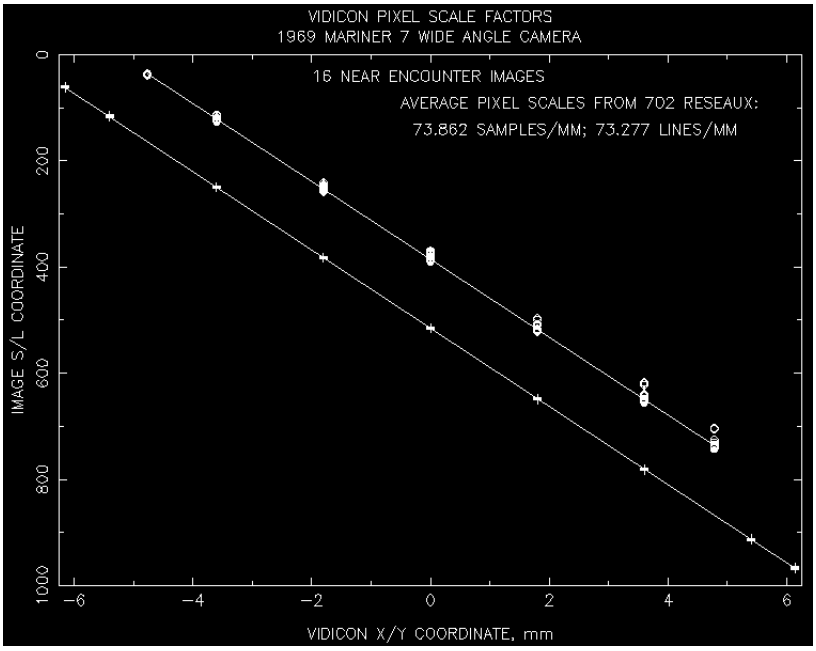

Figure 9: The Mariner 7 Near Encounter Wide Angle reseau sample/line image coordinates were plotted against their x,y mm focal plane locations to determine *a priori* values of K_{sx} and K_{ly}. Image 7N11 is missing lines that gives its reseaux erroneous image locations that show up as outliers in the upper data used for line scale.

Table 2: Comparing the partial derivatives computed using the analytic expressions vs numerically differenced values. The partial derivatives are only dependent on image location and not on any specific image.

Partial	Analytic	Differenced	Analytic	Differenced
$\partial(s,l)/\partial(K_{sx})$	-6.1520	-6.1520	0.0000	0.0000
$\partial(s,l)/\partial(K_{sy)}$	-3.6000	-3.6000	0.0000	0.0000
$\partial(s,l)/\partial(K_{lx})$	0.0000	0.0000	-6.1520	-6.1520
$\partial(s,l)/\partial(K_{ly)}$	0.0000	0.0000	-3.6000	-3.6000
$\partial(s,l)/\partial(s_0)$	1.0000	1.0000	0.0000	0.0000
$\partial(s,l)/\partial(l_0)$	0.0000	0.0000	1.0000	1.0000

Physics and Astronomy Department
4400 University Drive 6C3
Fairfax, VA 22030
Tel: +1 703 225-9080; Fax: +1 703 993-1296
tduxbury@gmu.edu

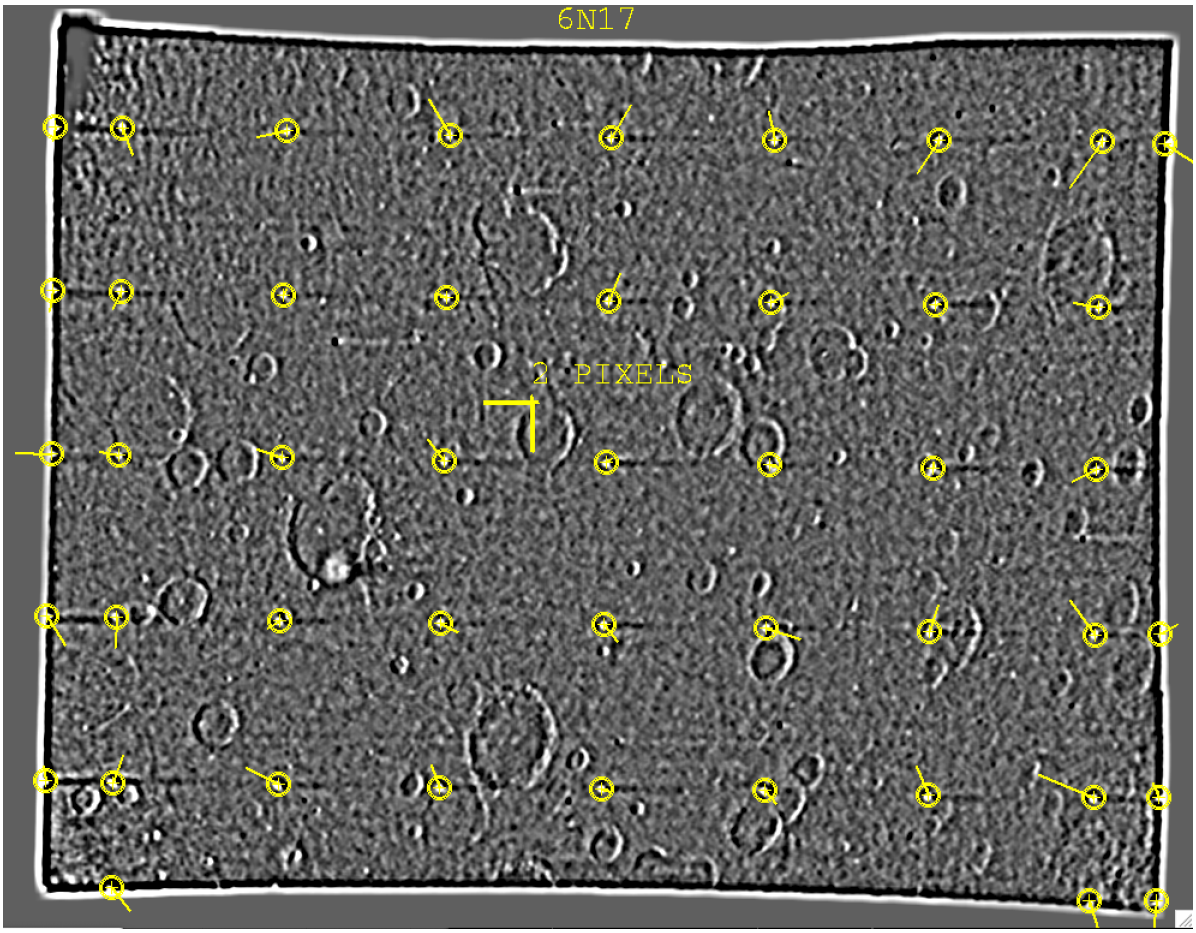

Figure 10: Near Encountyer image 6N17 was high pass filtered, its reseau locations were automatically measured using the weights in Figure 4 and the differences between the predicted and measured reseau locations (residuals) are plotted after the camera vidicon model was determined. The residual statistics had a zero mean and a standard deviation of less than 1 pixel (1-σ).

Table 3: Mariner 6 Near Encounter NA camera geometric model parameters

PICNO	# RES	K_{sx}	K_{sy}	K_{lx}	K_{ly}	s_0	l_0
6N02	47	74.1727	-0.3261	0.2062	73.6731	516.50	387.16
6N04	49	74.1897	-0.2860	0.2634	74.0382	516.76	387.90
6N06	53	74.1937	-0.3078	0.2875	74.1359	516.75	388.36
6N08	51	74.1357	-0.3126	0.2971	74.2663	516.48	388.20
6N10	48	74.1599	-0.3143	0.3209	74.2428	516.29	388.17
6N12	49	74.1302	-0.2899	0.1803	73.8652	516.27	386.55
6N14	52	74.1334	-0.3230	0.2875	74.1446	516.39	387.96
6N16	50	74.1363	-0.3093	0.2663	74.2330	516.43	387.75
6N18	51	74.1230	-0.3089	0.2970	74.2049	516.51	388.03
6N20	49	74.1368	-0.3392	0.2996	74.0020	516.47	386.61
6N22	45	74.1227	-0.4035	0.3799	73.7049	516.18	386.10
6N24	27	74.1837	-0.1043	0.1582	63.6043	516.83	334.87
6NAV	11	74.1486	-0.3201	0.2805	74.0464	516.46	387.53

Physics and Astronomy Department
4400 University Drive 6C3
Fairfax, VA 22030
Tel: +1 703 225-9080; Fax: +1 703 993-1296
tduxbury@gmu.edu

Figure 11: Each Near Encounter image was simulated by illuminating the global MOLA digital terrain model (DTM) of Mars. The level-2 6N17 EDR image is on the left and the MOLA simulated image is on the right.

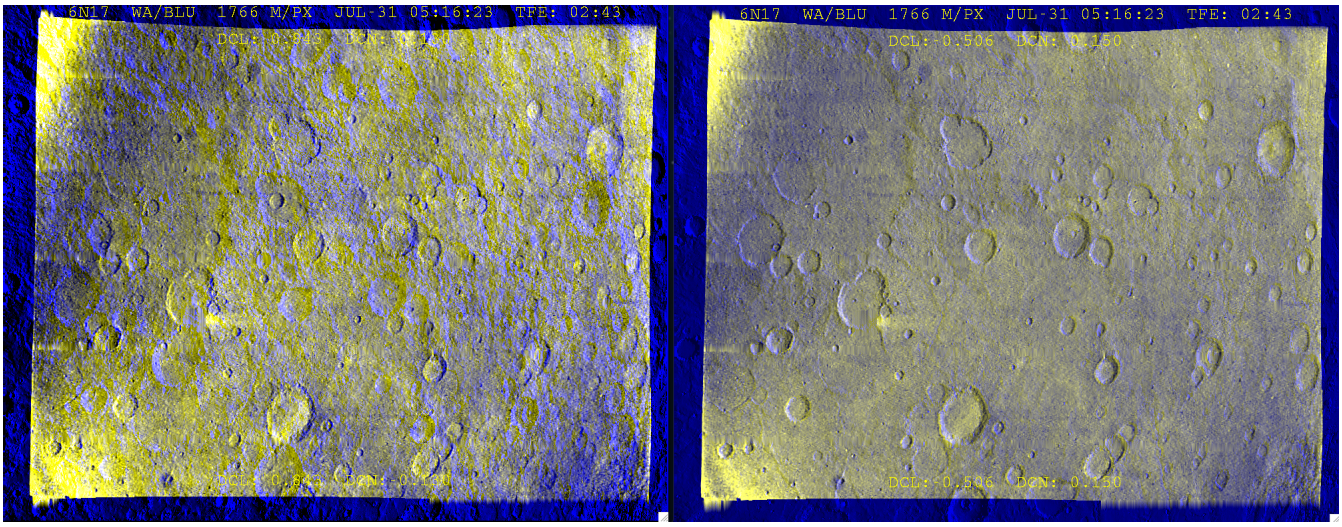

Figure 12: The Mariner 6 and 7 Narrow and Wide Angle camera focal lengths and pointing were determined by registering the simulated MOLA images with the actual level-2 EDR images by varying camera pointing and focal length. The left image shows when the actual and simulated images are not registered. They were registered on the right by changing camera pointing only, verifying the pre-flight values of focal length.

Physics and Astronomy Department
4400 University Drive 6C3
Fairfax, VA 22030
Tel: +1 703 225-9080; Fax: +1 703 993-1296
tduxbury@gmu.edu

Table 4: Mariner 6 Near Encounter WA camera geometric model parameters

PICNO	# RES	K_{sx}	K_{sy}	K_{lx}	K_{ly}	s_0	l_0
6N01	21	75.3127	-1.0704	1.3312	75.4870	512.20	386.77
6N03	34	75.4830	-1.2828	1.2204	75.4233	512.92	386.23
6N05	47	75.4148	-1.1520	1.1379	75.3593	512.86	386.05
6N07	48	75.3541	-1.1293	1.1268	75.3180	513.06	385.78
6N09	46	75.3999	-1.1758	1.1569	75.3587	512.86	386.07
6N11	46	75.3782	-1.1159	1.1598	75.3495	512.78	385.78
6N13	46	75.3725	-1.1501	1.1277	75.3706	512.81	385.97
6N15	44	75.3484	-1.0823	1.1475	75.4273	513.03	386.07
6N17	44	75.3744	-1.0758	1.1239	75.4088	512.90	385.67
6N19	46	75.4123	-1.0519	1.2005	75.2459	513.05	385.87
6N21	44	75.4209	-1.2038	1.0989	75.3027	512.77	386.21
6N23	37	75.3798	-1.1259	1.0879	68.1859	512.83	358.99
6N25	33	75.3562	-1.0739	1.1464	75.3699	512.95	386.17
6WAV	12	75.3856	-1.1303	1.1648	75.3684	512.85	386.05

Table 5: Mariner 7 Near Encounter NA camera geometric model parameters

PICNO	# RES	K_{sx}	K_{sy}	K_{lx}	K_{ly}	s_0	l_0
7N02	36	73.2555	-0.4452	0.6081	73.2213	514.48	388.42
7N04	62	73.2228	-0.4270	0.4915	73.1252	514.34	388.15
7N06	59	73.2598	-0.4146	0.4065	73.1984	514.52	387.87
7N08	59	73.2662	-0.4796	0.4778	73.2533	514.52	387.93
7N10	48	73.2582	-0.4425	0.4491	72.9247	514.42	386.13
7N12	49	73.2733	-0.5012	-0.1242	70.0364	514.15	373.82
7N14	60	73.1685	-0.4823	0.4694	72.6918	514.54	385.78
7N16	62	73.2037	-0.4309	0.5065	73.1816	514.69	387.79
7N18	59	73.2803	-0.4649	0.5182	73.2192	514.44	387.98
7N20	56	73.2394	-0.4612	0.4967	73.2005	514.50	388.17
7N22	58	73.2332	-0.4318	0.4545	73.1758	515.00	388.03
7N24	58	73.2402	-0.4698	0.3998	73.2172	514.56	388.15
7N26	46	73.2485	-0.4269	0.4529	73.0245	514.61	388.27
7N28	55	73.2398	-0.3973	0.4711	73.2018	514.88	388.16
7N30	54	73.2664	-0.3973	0.5268	73.1655	514.95	388.92
7N32	38	73.3198	-0.5224	0.4853	72.9704	515.00	388.41
7NAV	15	73.2468	-0.4462	0.4809	73.1181	514.63	387.88

Physics and Astronomy Department
4400 University Drive 6C3
Fairfax, VA 22030
Tel: +1 703 225-9080; Fax: +1 703 993-1296
tduxbury@gmu.edu

Table 6: Mariner 7 Near Encounter WA camera geometric model parameters

PICNO	# RES	K_{sx}	K_{sy}	K_{lx}	K_{ly}	s_0	l_0
7N01	19	73.9635	-0.1181	-0.2727	73.7475	515.17	387.01
7N03	30	73.9111	0.0492	-0.2446	73.7468	515.09	386.90
7N05	36	74.0003	0.1314	-0.2230	73.6373	514.91	386.89
7N07	54	73.8971	0.1399	-0.1582	73.6196	514.98	387.13
7N09	55	73.8501	0.1096	-0.2120	73.3219	514.91	386.35
7N11	46	73.8627	0.1369	-0.1351	69.6339	514.95	371.07
7N13	55	73.8829	0.0933	-0.2780	73.5116	514.92	387.05
7N15	38	73.8845	0.2048	-0.4093	73.1165	514.71	376.48
7N17	46	73.8510	0.2191	-0.1148	73.5308	514.92	386.99
7N19	38	73.8158	0.2253	-0.1733	73.5235	515.05	386.69
7N21	27	73.8633	0.1377	-0.2270	73.5998	515.59	386.63
7N23	52	73.8053	0.0637	-0.2165	73.5372	515.07	386.57
7N25	51	73.8319	0.0675	-0.1878	73.5570	515.09	387.14
7N27	59	73.8324	0.1196	-0.2206	73.4984	514.93	387.00
7N29	51	73.8525	0.1297	-0.2091	73.5819	515.06	386.87
7N31	45	73.8604	0.0878	-0.2642	73.6787	515.29	388.33
7WAV	15	73.8735	0.1107	-0.2274	73.5472	515.05	386.27

Table 7: Mariner 6 and 7 NA camera optical model parameter values

SPACECRAFT	f, mm	x_o, mm	y_o, mm	α_1, mm^{-2}	α_2, mm^{-4}
M'6	505.41	0.0	0.0	0.0	0.0
M'7	502.66	0.0	0.0	0.0	0.0